HHS Public Access

Author manuscript

Clin Exp Allergy. Author manuscript; available in PMC 2021 February 01.

Published in final edited form as:

Clin Exp Allergy. 2020 February ; 50(2): 198–212. doi:10.1111/cea.13538.

Eosinophil Cytolysis on Immunoglobulin-G Is Associated with Microtubule Formation and Suppression of Rho-Associated Protein Kinase Signaling

Stephane Esnault[1,*], **Jonathan P Leet**[1,*], **Mats W Johansson**[2], **Karina T Barretto**[2], **Paul S Fichtinger**[1], **Frances J Fogerty**[2], **Ksenija Bernau**[1], **Sameer K Mathur**[1], **Deane F Mosher**[2,3], **Nathan Sandbo**[1], **Nizar N Jarjour**[1]

[1]University of Wisconsin-Madison School of Medicine and Public Health, Department of Medicine, Division of Allergy, Pulmonary and Critical Care Medicine, Madison, WI, USA.

[2]Department of Biomolecular Chemistry, Madison, WI, USA.

[3]Department of Medicine, Division of Hematology and Oncology, Madison, WI, USA.

Abstract

Background—The presence of eosinophils in the airway is associated with asthma severity and risk of exacerbations. Cell-free eosinophil granules are found in tissues in eosinophilic diseases, including asthma. This suggests that eosinophils have lysed and released cellular content, likely harming tissues.

Objective—The present study explores the mechanism of CD32- and αMß2 integrin-dependent eosinophil cytolysis of IL3-primed blood eosinophils seeded on heat-aggregated immunoglobulin G (HA-IgG).

Methods—Cytoskeletal events and signaling pathways potentially involved in cytolysis were assessed using inhibitors. The level of activation of the identified events and pathways involved in cytolysis was measured. In addition, the links between these identified pathways and changes in degranulation (exocytosis) and adhesion were analyzed.

Results—Cytolysis of IL3-primed eosinophils was dependent on production of reactive oxygen species (ROS) and downstream phosphorylation of p-38 MAPK. In addition, formation of microtubule (MT) arrays was necessary for cytolysis and was accompanied by changes in MT dynamics as measured by phosphorylation status of stathmin and microtubule-associated protein 4 (MAP4), the latter of which was regulated by ROS production. Reduced ROCK signaling preceded cytolysis, which was associated with eosinophil adhesion and reduced migration.

Conclusion and Clinical Relevance—In this CD32- and αMß2 integrin-dependent adhesion model, lysing eosinophils exhibit reduced migration and ROCK signaling, as well as both MT

Corresponding Author: Address correspondence and reprint requests to Stephane Esnault; Division of Allergy, Pulmonary and Critical Care Medicine, Department of Medicine; 600 Highland Avenue, CSC K4/928; University of Wisconsin, School of Medicine and Public Health; Madison, WI 53792-9988; sesnault@wisc.edu; Tel: +1 608-265-8938; FAX: +1 608-263-3104.
*Both authors participated equally to the work

Data Availability

All the data used in this manuscript are available to the public.

dynamic changes and p-38 phosphorylation downstream of ROS production. We propose that interfering with these pathways would modulate eosinophil cytolysis and subsequent eosinophil-driven tissue damage.

Keywords

Eosinophil; cytolysis; degranulation; adhesion; priming; IL3; immunoglobulin-G; microtubule

Introduction

Eosinophilic severe asthma is characterized by exacerbations, eosinophilic inflammation, and lack of disease control [1]. In asthma, eosinophilia is strongly associated with type-2 cytokine production, including IL5 [2]. IL5 regulates eosinophil differentiation and activation; its production is highly upregulated in the airways after an allergen challenge and its receptor is almost exclusively present on eosinophils and basophils/mast cells [3–6]. Therefore, humanized monoclonal anti-IL5, or anti-IL5 receptor, antibodies have been developed to reduce eosinophilia. These therapies significantly decrease blood eosinophil count, but have a more modest effect on airway eosinophils [7–9]. We have recently shown that an injection of anti-IL-5 (mepolizumab) in subjects with mild asthma dramatically reduced blood and airway eosinophilia in bronchoalveolar (BAL) fluids after an allergen challenge [10]. Yet, in these patients, despite significant reduction of BAL eosinophils, we observed intense eosinophil toxic protein deposition and intact cell-free eosinophil granules in the airway tissue obtained via bronchial biopsies done following segmental allergen challenge in patients who had been pre-treated with anti-IL5 [10]. These data suggest significant eosinophil lysis in lung tissue, and potential implication of other pro-eosinophilic cytokines such as GM-CSF and IL3.

These findings are supported by several publications that reported presence of lysed eosinophils and cell-free granules in patients with atopic dermatitis and nasal polyps [11–13]. Furthermore, the number of extracellular eosinophil granules in lung tissue correlates with epithelial damage after allergen challenge [14]. Thus, although cytolysis of eosinophils in tissue is a mechanism for clearance of eosinophils (as proposed by Uller *et al.* [15]), the products of cytolysis may cause lingering damage by release of soluble mediators and cell-free intact granules, the latter of which can further release toxic proteins and other mediators, independently of intact eosinophils [16].

Several recent studies have described the formation of extracellular DNA traps by eosinophils [17, 18], which could be linked to the process of cytolytic cell-death leading to release of extracellular free eosinophil granules [19, 20]. More recently, extracellular crystals of Charcot-Leyden crystal protein (CLC) released upon cytolysis have been shown to activate the type-2 immunity [21]. Thus, products of lysed eosinophils likely contribute to eosinophilic inflammation. A previous analysis of intracellular events during non-apoptotic eosinophil death indicated that upon adhesion via αMß2 integrin to surfaces coated with the iC3b form of complement C3 and highly concentrated IgG, the eosinophil dies over an hour by necroptosis [22]. In this study, activation of markers of necroptosis was upstream of a signaling transduction pathway from phosphatidylinositol 3’-kinase (PI3K) to p38 mitogen-

activated protein kinases (MAPK), and the production of ROS by dihydronicotinamide-adenine dinucleotide phosphate (NADPH) oxidase [22].

We have previous developed an *in vitro* model of eosinophilic degranulation that recapitulates an airway eosinophilic-like phenotype responding to a biologically relevant extracellular cue found in the asthmatic airway. In this model, blood eosinophils are stimulated with long-term IL3 to induce a phenotype that is similar to intact airway eosinophils obtained after an *in vivo* segmental allergen challenge [23, 24]. In this model also, neutralizing antibodies against either CD32 or αMß2 integrin totally blocked eosinophil attachment and degranulation (EDN release) on heat-aggregated (HA)-IgG [23]. In contract to IL3, short or long-term treatment with IL5 does not result in a similar phenotypic shift, and results in rapid loss of surface IL5 receptor and downstream signaling [23–27]. Notably, antigen-bound or aggregated IgG is a relevant activator of eosinophils, [28, 29] because IgG is present in human airways and allergen-specific IgG correlates with EDN levels in sputum of asthmatic patients [30, 31], and IgG complexed with eosinophil peroxidase (EPX) and other autologous cellular components is present in airways of asthma subjects [32]. Importantly, we have observed that the interaction of *in vitro*-IL3-primed blood and *in vivo*-primed airway eosinophils with HA-IgG leads to an apparent cell death by cytolysis [23, 27]. Therefore, in this study, we sought to determine the key intracellular events implicated in the cytolytic death of IL3-primed eosinophils plated on HA-IgG.

Materials and Methods

Subjects and eosinophil preparation

The study protocol was approved by the University of Wisconsin-Madison Health Sciences Institutional Review Board. Informed written consent was obtained from subjects prior to participation. Peripheral blood eosinophils were obtained from allergic subjects with and without mild asthma. As previously described [23], eosinophils were purified by negative selection. Eosinophils were cultured at 1×10^6/ml in complete medium (RPMI 1640 plus 10% fetal bovine serum) with IL3 (2 ng/ml) for 20 hours, and were then washed and cultured with complete medium (no IL3) on heat-aggregated IgG (HA-IgG or IgG) or without IgG as previously described [23]. More detailed materials and methods are in the Supplemental Information section.

Reagents

Recombinant human (rh) IL3 was purchased from BD Biosciences (San Jose, CA, USA). Human serum IgG and phorbol myristate acetate (PMA) were from Sigma-Aldrich (St. Louis, MO). The following reagents with their final concentration were used on eosinophils: diphenyleneiodonium (DPI; 5μM; Selleckchem, Houston, TX, USA), L-N^G-monomethyl arginine citrate (L-NMMA; 10μM; Cayman Chemical, Ann Arbor, MI, USA), GSK843 (10μM; Aobious, Gloucester, MA, USA), necrosulfonamide (10μM; Calbiochem, Millipore Sigma, Burlington, MA, USA), benzyloxycarbonyl-Trp-Glu(OMe)-His-Asp(OMe)-fluoromethylketone (Z-WEHD-FMK; 5μM; Enzo Life Science, Farmingdale, NY, USA); (Z-VAD-FMK; 5μM; InvivoGen, San Diego, CA, USA), colchicine (1μM; Calbiochem), nocodazole (1μM; Calbiochem), cytochalasin-D (1μM; Calbiochem), Y27632 (10μM;

Calbiochem), 14–22-amide, myristoylated (4μM; Tocris-Bio-Techne Corporation, Minneapolis, MN, USA), SB203580 and SB202474 (0.5μM; Calbiochem), U0126 and U0124 (2μM; EMD Millipore), JNK inhibitor II (5μM; Calbiochem), LY294002 (10μM; BioGems, Westlake Village, CA, USA).

Cytolysis measurement of eosinophils on heat aggregated IgG (HA-IgG)

At the indicated times and at the concentration recommended by the provider, 20 μl of bis-alanyl-alanyl-phenylanlanyl-rhodamine 110 (R110; CytoTox-Fluor™ Cytotoxicity Assay, Promega, Madison,WI) was added in each well for 30 min to measure loss of membrane integrity by fluorescence (Fluo) ($485nm_{Ex}/520nm_{Em}$). For experiments with inhibitors, inhibitor was added to cells after the 20 hours of IL3 priming, and 15 minutes before seeding on coated HA-IgG (IL3IgGInh). Vehicles (DMSO, ethanol) used to prepare the inhibitors or specific analogs were used as controls (IL3IgGCon). Percentage inhibition of cytolysis was calculated as follows: [1-((FluoIL3IgGInh-FluoIL3)/ (FluoIL3IgGCon-FluoIL3))] X 100.

Microscopy for time –lapse

Peripheral blood eosinophils were cultured at 1×10^6/ml in complete medium, with IL3 (2 ng/ml) for 20 hours. After 20 hours with IL3, eosinophils were washed and suspended at 2×10^5/ml in fresh medium (no cytokine). Two ml of the cell suspension was added into glass bottom culture 35 mm diameter Petri dishes with 14 mm glass diameter No. 1.0 coverslip (MatTek, Ashland, MA, USA) which had been incubated overnight with HA-IgG (10μg/ml; 500μl/well) and saturated with 0.1 % gelatin for 30 minutes at 37°C. Cells were imaged between 0 to 5 hours after seeding on HA-IgG-coated dishes. Time-lapse images were captured in a DMi8 inverted wide-field microscope (Leica, Buffalo Grove, IL, USA) with a motorized stage and Tokei Hit temperature- and CO2-controlled chamber using a 63x oil immersion objective, at the University of Wisconsin-Madison Optical Imaging Core Facility. Live-cell images of 1 frame/5 seconds were acquired using DIC optics on Leica Application Suite X (LASX) and Metamorph software.

Total cellular EDN measurement and degranulation on heat aggregated IgG (HA-IgG)

Supernatant fluids were analyzed by ELISA for EDN release. The human EDN ELISA used (MBL, Woburn, MA) has a minimum detection limit of 0.62 ng/ml.

Adhesion measurement of eosinophils on heat aggregated IgG (HA-IgG)

Eosinophils were primed with IL3 (2 ng/ml) for 20 hours in complete medium. Then eosinophils (5×10^3 per well in 100 ul) were plated in wells of a 96 well-plate previously coated with aggregated IgG (IL3IgG) or without IgG (IL3). All conditions were performed in quadruplicate, and the plate was incubated for 2 hours at 37°C in 5% CO_2. Then, cells were fixed with 4% paraformaldehyde (PFA) in PBS for 10 minutes at room temperature, and permeabilized by adding 0.1% Triton X-100 in PBS. The wells were blocked by adding Odyssey Blocking Buffer in PBS (LI-COR) for 30 minutes. After removing blocking buffer, 50ul/well of Cell Tag 700 diluted 1:500 in blocking buffer was added and the plate was placed on a plate shaker for 1 h protected from light. The Cell Tag 700 was then removed and the plate was washed 5 times with 0.1% Tween 20 in PBS. The wash buffer was then

completely removed and the plate was either immediately imaged or stored at 4°C in a plastic bag protected from light for imaging the following day. Imaging was performed using the LI-COR CLx with a 3.5 um focus offset and scanned at medium quality with 84 um resolution. Intensity of Cell Tag 700 staining was measured in the 700 nm channel and quantified using Image Studio 5.2 software and the 96 well plate In-Cell Western analysis settings. Cell Tag 700 is designed specifically for normalizing cell number for In-Cell Western quantification, thus the intensity of staining correlates with the number of eosinophils adhered to a given plate well.

Reactive oxygen species (ROS) measurement

Eosinophils (1×10^6/ml per well) were primed with IL3 (2 ng/ml) for 19 hours in complete medium before addition of dihydrorhodamine-123 (5μM; Molecular Probes, Eugene, OR, USA-Invitrogen™). Then, cells were washed and seeded on HA-IgG (IL3IgG) or without IgG (IL3) in 96-well plate in quadruplicate. The indicated inhibitors or vehicle only or analog control were added on cells 15 minutes before seeded on IgG. Intracellular ROS production was measured by fluorescence ($485nm_{Ex}/520nm_{Em}$) at the indicated time points. Fluorescence measured in medium only (no cells) was subtracted from the values shown. As a positive control for ROS production, IL3-primed eosinophils were treated with PMA (100 ng/ml) for the indicated times.

Oxidative activity release by eosinophils

Eosinophils were primed with IL3 (2 ng/ml) for 20 hours and were seeded (IL3IgG) or not (IL3) on HA-IgG for the indicated times. Cell supernatant fluids were stored at −80°C until processed. Oxidative activity in the culture media was measured by chemiluminescence (emission at 430 nm) using Acridan Lumigen PS-3 (Lumigen ECL Plus (PS-3; Lumingen, MI ,USA) as described by Uy et al [33]. Briefly, 20 μl of culture medium and 40 μl of PBS were added in quadruplicate in wells of a 96-well plate. Lumigen reagent was prepared as recommended by the provider and 50 μl of the reagent was added in each well. Luminescence was read after 8 minutes at 430 nm. Luminescence measured in control medium was subtracted from values obtained with culture media.

Microscopy

Peripheral blood eosinophils were cultured at 1×10^6/ml in complete medium, with IL3 (2 ng/ml) for 20 hours. After 20 hours with IL3, eosinophils were washed and suspended at 0.6×10^6/ml in fresh medium (no cytokine) and 500 μl was added to acid-washed coverslips in a 24-well plate, which had been incubated overnight with or without HA-IgG (10μg/ml; 500μl/well) and saturated with 0.1 % gelatin for 30 minutes at 37°C. For experiments with inhibitors, inhibitor was added on cells after IL3 priming, and 15 minutes before seeding on IgG. Vehicles (DMSO, ethanol) used to prepare the inhibitors or specific analogs were used as controls. After 5 hours of incubation at 37°C, coverslips were fixed with 3.7% PFA and quenched with glycine. Eosinophils were permeabilized using 0.05% Triton X-100/PBS for 4 min at 37°C. Coverslips were washed with PBS, incubated with 10% BSA for 1 hour, and incubated for 12–15 hours at 4 °C in primary antibodies diluted in 2% BSA, 0.1% SDS in PBS. The primary antibodies used were rabbit anti-CD11b (Abcam, Cambridge, MA) diluted 1:200 and mouse monoclonal anti-α-tubulin (Sigma-Aldrich) diluted 1:500.

Coverslips were washed in PBS and incubated for 1h at room temperature with Alexa Fluor 488–conjugated donkey anti-rabbit IgG and Alexa Fluor 555-conjugated donkey anti-mouse IgG secondary antibodies (both from Thermo Fisher Scientific, Madison, WI) diluted 1:1000 in 2% BSA, 0.1% SDS in PBS. After incubation with 4′,6-diamidino-2-phenylindole (DAPI), coverslips were mounted on slides, and sequential 0.3-μm z-step images were acquired using Nikon A1R-Si+ Confocal (60× oil objective) at excitation/emission wavelengths of 409/450, 488/525, and 561/ 595 nm. Laser power settings and conversion gains were kept constant and images were reconstructed post-acquisition using NIS Elements AR v4.30 software and are displayed as maximal intensity projections (signal from all slices).

Western-blot

Eosinophils (1×10^6/ml per well) were primed with IL3 (2 ng/ml) for 20 hours and were seeded on HA-IgG for the indicated times. Cells were lysed directly in Laemmli buffer (10% SDS plus ß-mercaptoethanol), before boiling and loading onto 8% or 10% SDS–polyacrylamide gels. Immunoblotting was performed as previously described [34]; briefly, samples were subjected to polyacrylamide gel electrophoresis at 150V for 1 hour and then transferred at 100V for 1.5 hour. Western blots were subsequently incubated with desired primary antibodies: anti-ß-actin from Sigma Aldrich, anti-cofilin from Santa Cruz Biotechnology, anti-phospho-cofilin from Cell Signaling Technology (Danvers, MA, USA), anti-phospho-p38 from Genetel Laboratories (LLC, Madison, USA), anti-phospho-MAP4 from ThermoFisher Scientific (Rockford, IL, USA) and anti-phospho-stathmin from Cell Signaling. Then the appropriate (anti-mouse or anti-rabbit) HRP-conjugated secondary antibodies (Calbiochem) were utilized. Immunoreactive bands were visualized using ECL reagents and GE LAS4000 chemiluminescence imager (GE Healthcare, Little Chalfont, UK). Bands were quantified using ImageJ (https://imagej.nih.gov/ij/).

Cell motility assay

Purified blood eosinophils suspended in 1×10^6/ml in complete medium were cultured with IL3 (2 ng/ml) for 20 h. Cell motility was assessed in a bead clearing assay as previously described [35–37] with the following modifications. Wells had been coated overnight at 37ºC with HA-IgG (10 μg/ml, 50 μl per well), or rh periostin (R&D Systems, Minneapolis, MN, 5 μg/ml in Tris-buffered saline, 100 μl per well), or were not coated. Then, all wells were blocked with 0.1% gelatin in HBSS for 30 minutes at 37ºC, and 1-μm-diameter Polybeads were added to the wells. IL3-primed eosinophils were washed, diluted to 20,000/ml in RPMI-20% FBS without cytokine, pretreated or not with Y27632 for 10 minutes, and 50 μl (i.e., 1,000 cells) was added to each well and incubated for 2 hours at 37ºC. Wells were viewed in an Eclipse Ti inverted microscope (Nikon, Melville, NY, USA), images were acquired and exported using NIS-Elements AR, and percentage of area covered by migration tracks was quantified using ImageJ (https://imagej.nih.gov/ij/).

Statistical analyses

Statistical analyses were performed using the SigmaPlot 13.0 software package (Systat Software, Inc., San Jose, CA, USA). Differences between two groups were analyzed using the paired Student's *t*-test or *t*-test without or after log10 transformation. One-Way ANOVA

followed by the Holm-Sidak method was used to compare more than two groups. $P < 0.05$ was considered statistically significant. Three to six different donors with or without asthma were used for each condition. In Figure 1D, the significant p value was adjusted for multiple comparisons using Bonferroni Correction.

More detailed Material and Methods is described in the Supplemental Information ***section***

Results

Inhibition of reactive oxygen species production, microtubule formation, actin formation, or p38 or PI3K signaling prevents eosinophil cytolysis on IgG

Demonstration of IL3-primed blood eosinophil cytolysis on IgG and its kinetics are shown in Figure 1. Significant cytolysis was observed at 4 hours on IgG after priming with IL3 but not after priming with IL5 (Figure 1A). Figure 1B shows three time-lapse panels of a typical motionless IL3-primed cell losing membrane integrity between 3 and 4 hours on IgG as indicated by the black arrows. To evaluate the degree of cell death on IgG at 4 hours, eosinophils were treated with a cytotoxic dose of PMA for 4 hours to provide quantification for 100% cell death. Figure 1C indicates that ~50 % of maximal measurable cell death of IL3-primed eosinophils on IgG was reached after 4 hours.

Next, we screened for cell-death-relevant intracellular events involved in cytolysis by treating eosinophils with inhibitors (Figure 1D) after IL3 priming beginning 15 minutes before seeding on IgG for 5 hours. Note that cytolysis after IL3-priming reached a slightly higher level at 5 h (12460±1350, n=10) than at 4 h on IgG (10479±955, n=4). As shown in Figure 1D, inhibitors of ROS production (DPI), MT formation (nocodazole), actin polymerization (cytochalasin-D), mitogen-activated protein kinase (MAPK)-p38 (SB203580) and phosphoinositide 3-kinase (PI3K) (LY294002) signaling implicated these processes or enzymes as being required for eosinophil cytolysis. In contrast, Rho-associated, coiled-coil containing protein kinase (ROCK) inhibition (Y27632) enhanced cytolysis. Statistical significance for the effect on cytolysis remained for all inhibitors mentioned above but for Y27632 after p value correction ($p<0.0035$) for multiple comparisons. Inhibitors of nitric oxide synthase (L-NMMA), caspases 1, 4, 5 and 8 (Z-WEHD-FMK), protein kinase A (PKA) (14–22-amide) and the MAPKs ERK (U0126) and JNK (JNK inhibitor II) indicated that these processes or enzymes are not involved in IgG-induced cytolysis. In addition and in contrast to the reaction of unprimed eosinophils with surfaces coated with concentrated IgG and iC3b [22], inhibitors of necroptosis effectors RIPK3 (GSK843) and MLKL (necrosulfonamide) had no effect on cytolysis (Figure 1D). Finally, the implication of apoptosis in cytolysis in this model was evaluated by microscopic observation using the pan-caspase inhibitor, Z-VAD-FMK (5μM), and as expected [22], apoptosis did not appear to be involved in cytolysis (data not shown).

PI3K and actin polymerization are implicated in non-cytolytic eosinophil degranulation on IgG

Release of mediators from granules of live eosinophils occurs by exocytosis or piecemeal release [38, 39] and was measured in IL3-primed eosinophils on IgG using EDN release into

the extracellular compartment. Contrasting with release of intact granules by cytolysis, eosinophil release of granule proteins was detected soon after adhesion (30 minutes, p=0.005 compared to no IgG at 6 hours) and continued linearly up to 6 hours (Figure 2A), indicating decoupling of degranulation and cytolysis. Use of specific inhibitors indicated that PI3K (Figure 2B) is required for and F-actin polymerization (cytochalasin-D) (Figure 2C) is implicated in such non-cytolytic degranulation. Inhibitors of ROS (Figure 2D), MT formation (Figure 2E), p38 (Figure 2F) or ROCK (Figure 2B) did not affect eosinophil degranulation.

PI3K signaling is required for eosinophil adhesion on IgG

Previously, measurement of adherent eosinophils was determined by quantification of a cellular protein such as EPX (a.k.a. EPO) [40]. Because in our model eosinophils have likely lost a large amount of EPX after 2 hours on IgG (Figure 2A), we used a different and original approach consisting of quantifying eosinophils using fluorescence of a non-specific cellular compound, CellTag 700 Stain. In Figure 3A (top panel), representative culture wells in quadruplicate are shown demonstrating adherent cells after 2 hours on IgG (IL3IgG) or without IgG (IL3). A very low degree of adhesion was detected (Figure 3A, bottom panel) in the absence of IgG (IL3), while the presence of coated IgG (IL3IgG) highly and very significantly increased eosinophil adhesion. The PI3K inhibitor strongly inhibited eosinophil adhesion while inhibitors of actin polymerization, MT formation, ROCK or p38 signaling did not affect adhesion (Figure 3B).

Based on these observations, subsequent study of cytolysis focused on the analysis of events that impact cytolysis once eosinophils had adhered to HA-IgG. These included ROS production, p38 phosphorylation, MT formation and ROCK signaling.

Eosinophils on IgG quickly produce large amount of ROS

Eosinophils on HA-IgG increased the rate of ROS production rapidly and linearly comparable to PMA-treated cells, which were used as a positive control (Figure 4A). As would be expected [22], ROS production was completely inhibited by the NADPH oxidase inhibitor, DPI (Figure 4B). DPI also inhibited the IgG-induced increase in ROS into the extracellular compartment (Figure E1). In contrast, an inhibitor of MT formation (colchicine, Figure 4C), actin polymerization (cytochalasin-D, Figure 4D), ROCK (Y27632, Figure 4E) or p38 (SB203580, Figure 4F) signaling had no effect on ROS production. The inhibitor of PI3K (LY294002), which strongly inhibited adhesion (Figure 3B) also prevented most of the ROS production in cells (Figure 4E). These results indicate that ROS is produced downstream of adhesion; and independently of MT and actin formation, and ROCK and p38 signaling.

Eosinophils display microtubule (MT) arrays on IgG

Because both of the inhibitors of MT formation (colchicine and nocodazole) strongly inhibited cytolysis (Figure 1D), we performed immunohistochemistry for MT array formation in IL3-primed eosinophils on IgG. In Figure 5A (left image), staining for CD11b (α_M integrin, ITGAM) and tubulin reveals that IL3-primed eosinophils spread on IgG and displayed MT arrays. Cell membrane disruption was typically accompanied by loss of MT

organization and nuclear (DAPI) diffusion (Figure 5A; right image). Colchicine prevented the formation of MT arrays (Figure 5B), while the pro-cytolytic treatment with ROCK inhibitor (Y27632, Figure 1C) did not. Treatment with inhibitors of ROS production (DPI) or p38 signaling (SB203580), which were shown to reduce cytolysis (Figure 1D), did not prevent MT formation (Figure 5D/E). Taken together, these observations indicate that the presence of MT arrays per se is not sufficient to induce cytolysis and suggest a role for MT dynamics in cytolysis. MT dynamics are usually defined by rates of microtubule growth and shortening, and the frequencies of catastrophes and rescues [41, 42]. To demonstrate changes in events linked to MT growth and rescue frequency, we analyzed the phosphorylation status of two regulators of MT polymerization/depolymerization and catastrophe/rescue events, stathmin and MAP4 [41–43]. The functions of these two MT-associated proteins (MAPs) have not been studied in eosinophils, although we had previously shown, using a proteomic approach, that stathmin and MAP4 were present in resting and IL3-activated eosinophils [44, 45]. We thus analyzed the phosphorylation status of Ser38 of stathmin and Ser696 in MAP4 in IL3-primed eosinophils on HA-IgG compared to no HA-IgG. If MT growth and rescue frequency were increased on IgG, we would expect stathmin to be phosphorylated and MAP4 to be dephosphorylated [41–43]. Figure 6A shows that stathmin was indeed phosphorylated in IL3-primed eosinophils on IgG for 2 or 4 hours, and MAP4 was dephosphorylated at 4 hours. Inhibition of ROS production with DPI reversed MAP4 dephosphorylation after 3.5 hours on IgG, while inhibition of p38 (SB203580), MT formation (Nocodazole) and ROCK (Y27632) had no effect (Figure 6B/C). ROS production also seemed to inhibit stathmin phosphorylation, while no other analyzed pathways had a significant role in stathmin phosphorylation (Figure 6D). ROS inhibition did not change MAP4 or stathmin phosphorylation at an earlier time-point (2 h on IgG) (data not shown), indicating that ROS production acted on MT dynamics at the time when eosinophils lysed (3–4 h). Therefore, on IgG, eosinophils formed MT arrays and changed MAP phosphorylation status favoring MT growth and rescue events. Among the pathways analyzed, ROS production was the only regulator of the phosphorylation of MAPs.

Eosinophils phosphorylate p38 and dephosphorylate cofilin when on IgG

Since p38 and ROCK inhibitors decreased and increased eosinophil cytolysis, respectively (Figure 1D), p38 and ROCK signaling were quantified in IL3-primed eosinophils on IgG. Figures 7A and B show that p38 was quickly phosphorylated at Thr180 and Tyr182, while a downstream target of ROCK, cofilin, was dephosphorylated at Ser3 in eosinophils on IgG. As expected, the inhibitor of p38 (SB203580) significantly decreased p38 phosphorylation (Figure 7C). Interestingly, inhibition of ROS (DPI) almost completely prevented p38 phosphorylation (Figure 7D), indicating that ROS production is essential for p38 phosphorylation. Inhibition of MT polymerization (nocodazole) and ROCK signaling (Y27632) decreased and tended to increase p38 phosphorylation, respectively, although changes were small (Figure 7D). None of inhibitors of ROS production (DPI), p38 signaling (SB203580) or MT polymerization (nocodazole) altered cofilin phosphorylation (Figure 7E). Of note, the trend ($p=0.12$) to a minute effect of ROCK inhibitor (Y27632) on its downstream target, cofilin dephosphorylation, compared to its vehicle (DMSO; Figure 7F) was probably due to the initial low detection level of cofilin phosphorylation in eosinophils when interacting with IgG (Figure 7A). We may also speculate that ROCK inhibition with

Y27632 enhanced cytolysis on IgG (Figure 1D) via other known ROCK substrates involved in cell polarization, contraction, elongation and migration [46].

While p38 signaling seemed easily modulated, particularly by ROS production, none of the manipulations reversed the reduction of ROCK signaling (i.e., cofilin dephosphorylation) (Figure 7D/E). Notably, it has been previously shown that Rho-associated protein kinase (RhoA)/ROCK signaling is essential for eosinophil migration [47]. Therefore, we proposed that migration arrest and lack of motion might be an important event preceding or concomitant with cytolysis. To quantify the hypothesized lack of eosinophil migration on IgG, we used a previously described bead-based cell-motility assay [36, 37]. Figure E2 shows that IL3-primed eosinophils in the absence of IgG (IL3) displayed some migration, whereas in presence of IgG (IL3IgG) lack of migration or only small circular traces but no migration tracks were observed. Furthermore, although not statistically significant, treatment with the anti-ROCK signaling compound (Y27632) caused a trend to further attenuation of cell movement (Figure E2B). Small circular movements of eosinophils on IgG was further demonstrated in Video 1, where cells have a typical small circular movement. Additionally, Video 1 shows an occasional early event on IgG, an eosinophil that quickly adhered and remained motionless.

Discussion

While the damaging consequences of eosinophil cytolysis via release of intracellular mediators and intact cell-free granules are recognized in eosinophilic diseases [12–15], there is little knowledge of the mechanisms leading to loss of the integrity of eosinophil cytoplasmic membrane. Our study reveals several cytoskeletal events and intracellular pathways required for lysis of primed eosinophil following interaction with surface-bound HA-IgG via CD32 and αMß2 integrin.

We found that the pathways leading to cytolysis include ROS production and p-38 phosphorylation. The identification of these two intracellular events in an eosinophil non-apoptotic death is in accordance with a recent study, which described unprimed eosinophils interacting with glass surfaces coated with a mixture of IgG and iC3b, a ligand for αMß2 [22]. However, we observed some notable differences compared to this previous study by Radonjic-Hoesli *et al.* In this previous report, cytolysis occurred in the first hour, whereas in ours there was a several-hour latency period. In addition, although both ROS and p-38 phosphorylation occur within minutes, we found that NADPH-dependent ROS production was upstream of p-38 phosphorylation rather than the opposite [22]. However, lack of both tight early kinetics to define the exact timing of p-38 phosphorylation and measurement of phosphorylation of all four p-38 proteins (p-38α, p-38ß, p-38γ are p-38δ) are limitations of this study. This may be important since the inhibitor used in this study is potent for p-38α and ß but has little to no effect on p-38γ and p-38δ [48, 49]. Furthermore, unlike this previous work, we did not detect any blockade of cytolysis by inhibition of necroptosis effectors, RIPK3 and MLKL. These discrepancies between the two studies may be due, at least partially, to our use of a long-term priming with IL3 as opposed to lack of priming and the use of freshly prepared eosinophils, and the use of different type and concentration of coated IgG. It is not known what model best mimics *in vivo* tissue eosinophil activation and

cytolysis. However, we believe that a period of priming *in vitro* is appropriate because it recapitulates *in vivo* events (i.e. after exposure to a relevant allergen), the change of cell phenotype from blood to airway eosinophil [50–52], and the activation of αMß2 integrin [53] as the cells move through the airway tissue. To demonstrate the importance of priming, we have recently shown, using a proteomic approach, that IL3 priming led to differential amounts of 1853 proteins and changes of phosphorylation at 7330 sites compared to unactivated eosinophils [44]. Furthermore, measuring adhesion along with degranulation (i.e. EDN release) and cytolysis allowed us to attribute a role for PI3K in adhesion rather than in cytolysis per se as proposed in the Radonjic-Hoesli *et al.* study, where PI3K was considered a messenger linking necroptosis to p38 phosphorylation upstream of ROS production [22]. Of note, the role of PI3K in eosinophil adhesion via αMß2 integrin is in accordance with previous studies by Sano *et al.* [54] and Barthel *et al.* [55]. Nevertheless, a limitation in our study is the lack of identification of ligand(s) for αMß2 integrin, which we know is required for eosinophil degranulation in this model [23], as well as the lack of examination of autophagy [22].

NADPH oxidase-derived ROS are well-known actors in cell death, particularly in granulocytes, including eosinophil cell death associated with DNA trap release [19]. Worth mentioning, although DNA trap formation occasionally occurred in our model (not shown), this event was not analyzed in our present study. The reason for the lack or rare observation of DNA traps in our model remains unknown but may be due to the use of a low concentration of IgG (10 μg/ml), the long-term priming, and the presence of 10% serum. It is also noteworthy that DNA trap release is not necessarily accompanied by cell death [20], indicating that cell cytolysis and DNA trap release can be two uncoupled events. In neurons, ROS can drive cell degeneration via cytoplasmic membrane oxidation [56], its connection with autophagy [57], and the disruption of cytoskeletal proteins leading to axonal fragmentation (reviewed in [58]). Here we found that MT formation is required for cytolysis, and we revealed that ROS likely control the phenomenon of MT polymerization/rescue by dephosphorylation of MAP4. Although the MT network has been implicated in polarization of activated eosinophils in suspension [59] and several eosinophil MAPs, including stathmin, are known to change phosphorylation state upon acute activation with IL5 [45, 60], no study has previously reported an analysis of MAP phosphorylation in relation to function in eosinophils. MAPs bind to MT and regulate their dynamics, growth, catastrophe and association with other molecular complexes [61]. MAP4 stabilizes microtubules primarily by preventing catastrophes and increasing rescue frequency [41], which define the dynamic instability of microtubule arrays, an important phenomenon for microtubule activity. Phosphorylation of MAP4 by p38 on Ser696 and Ser787 leads to microtubule disassembly [62]. This agrees with the dogma that phosphorylation of MAP4 induces its dissociation from microtubules [63]. Therefore, we propose that dephosphorylation of MAP4 in eosinophils on IgG is associated with its binding to MT and MT polymerization/rescue. In plants, ROS generation by NADPH oxidase along with p38-like MAPKs orchestrate MAP activities and the rearrangements of tubulin cytoskeleton [64]. Surprisingly, in eosinophils, while ROS enhanced p38 phosphorylation, p38 had no effect on MAP4 phosphorylation. The downstream target(s) of p38 accounting for eosinophil cytolysis remain unknown.

By binding microtubules, MAP4 can stabilize the microtubules by sterically blocking active microtubule-disassembling proteins, such as stathmin (a.k.a. Op18) [41]. Phosphorylation of stathmin mimics reduction of stathmin protein amount, which results in its release of bound tubulin heterodimers and enhanced polymerization activity and stability of the microtubules (reviewed in [42]). We found that eosinophils on IgG phosphorylate stathmin, and yet none of the pathways studied were involved in the change of stathmin phosphorylation status. On the contrary, inhibition of ROS enhanced stathmin phosphorylation, indicating that ROS reduce stathmin phosphorylation. Four phosphorylation stathmin sites have been identified and are important for inactivation of stathmin activity (reviewed in [42]). The pathway responsible for stathmin phosphorylation in eosinophils on IgG remains unknown. It is interesting to note that we recently observed in a proteomic analysis that IL3 priming of eosinophils for 20 hours was associated with decreased phosphorylation of MAP4 at Ser696 and increased phosphorylation of stathmin at Ser38,compared to resting eosinophils (supplemental spreadsheet 2 in [44]). These proteomic data suggest that IL3 priming already changes or conditions the phosphorylation states of MAP4 and stathmin before contact with IgG and ligand(s) for integrins.

The interactions among MT, actin and myosin, and their roles in degranulation and cytolysis as well as the role of migration arrest and ROCK signaling in these processes remain important questions for future investigations. As replicated here, actin polymerization is implicated in eosinophil degranulation (i.e. EDN release) [65]. However, unlike this previous study by Shamri *et al.*, we did not find a significant effect of MT polymerization on degranulation. This difference may be due to the use of a lower dose of MT polymerase inhibitor in our study. Therefore, although actin signaling seems more involved in degranulation and MT polymerization more involved in cytolysis, the cytoskeleton rearrangement in general may be implicated in both events. In another study, colchicine did not alter eosinophil viability when interacting with coated IgG [66]. The discrepancy between this previous study and our current work may be due to the use of fresh eosinophils, the lack of cell priming, and the marginal increase of cell death when eosinophils bound to monomeric IgG. In apoptotic cells, surface blebbing is observed upon activation of myosin II via caspase cleavage of ROCK, ultimately promoting cells breaks [67]. RhoA inhibition reduces migration in different cells [68], and inhibition of RhoA/ROCK pathway causes firm attachment of the rear part of eosinophils to its substrate and migration arrest [47]. Altogether, we may speculate that upon interaction with IgG, eosinophils quickly reduce ROCK signaling leading to migration inhibition and eventually total lack of motility, which along with important cytoskeleton dynamics ultimately causes cell membrane disruption.

In summary, our study supports the concept that when cytokine-primed eosinophils adhere via CD32 and αMß2 integrin in a PI3K-dependent manner, as it is likely to happen when they are in airway tissue, these eosinophils can quickly release their granular contents under the control of actin polymerization. Reduced ROCK signaling promotes limited movement of eosinophils on IgG, eventually reaching motility arrest. Concomitantly on IgG, MT arrays are dynamically formed while ROS production controls p38 phosphorylation and MAP4 dephosphorylation, the latter of which directs MT dynamics, ultimately leading to cytolysis and release of cell-free granules (Figure E3). We propose that these mechanisms and pathways participate in eosinophil cytolysis and the release of large amount of cellular

mediators and cell-free granules *in vivo* in tissues of subjects with asthma and other eosinophilic diseases.

Supplementary Material

Refer to Web version on PubMed Central for supplementary material.

Acknowledgements

The authors wish to thank the subject volunteers who participated in this study; Elizabeth McKernan, BS, of the Eosinophil Core facility (P.I., Sameer Mathur, M.D., Ph.D.) for blood eosinophil purification; the research nurse coordinators in the Clinical Core facility (P.I., Loren L. Denlinger, M.D., Ph.D) for subject recruitment and screening; and John Crooks for advice on photography of bead clearing motility experiments. We thank our statistician Kristine Lee, MS for her advice on some of the statistical analyses. Microscopy was performed at the University of Wisconsin-Madison Biochemistry Optical Core, which was established with support from the University of Wisconsin-Madison Department of Biochemistry Endowment. This work was supported by Program Project grant P01 HL088594 and Clinical and Translational Research Center grant UL1 TR002373 from the National Institutes of Health.

Conflict of Interest Statement: MWJ received a grant from Hoffmann-La Roche, received a speaker fee from and was an advisory board member for Genentech, and received consulting fees from Guidepoint Global; all these items were unrelated to the content of the present manuscript. All other authors have no relevant conflict of interest.

Abbreviations

CD32	receptor for Fc fragment of IgG, low affinity II (FCGRII)
DAPI	4′,6-diamidino-2-phenylindole
DPI	diphenyleneiodonium
EDN	eosinophil-derived neurotoxin
HA-IgG	heat-aggregated immunoglobulin G
MAP4	microtubule-associated protein 4
MAPK	mitogen-activated protein kinase
MT	microtubule
NADPH	dihydronicotinamide-adenine dinucleotide phosphate
PFA	paraformaldehyde
PI3K	phosphatidylinositol 3’-kinase
ROCK	Rho-associated, coiled-coil containing protein kinase
ROS	reactive oxygen species
SBP-Ag	segmental bronchoprovocation with an allergen

References

1. Busse W, Chupp G, Nagase H, Albers FC, Doyle S, Shen Q, Bratton DJ, Gunsoy NB, Anti-IL-5 treatments in patients with severe asthma by blood eosinophil thresholds: Indirect treatment comparison. J Allergy Clin Immunol 2019;143: 190–200 e20. [PubMed: 30205189]
2. Evans MD, Esnault S, Denlinger LC, Jarjour NN, Sputum cell IL-1 receptor expression level is a marker of airway neutrophilia and airflow obstruction in asthmatic patients. J Allergy Clin Immunol 2018;142: 415–23. [PubMed: 29103994]
3. Wilson TM, Maric I, Shukla J, Brown M, Santos C, Simakova O, Khoury P, Fay MP, Kozhich A, Kolbeck R, Metcalfe DD, Klion AD, IL-5 receptor alpha levels in patients with marked eosinophilia or mastocytosis. J Allergy Clin Immunol 2011;128: 1086–92 e1–3. [PubMed: 21762978]
4. Yasruel Z, Humbert M, Kotsimbos TC, Ploysongsang Y, Minshall E, Durham SR, Pfister R, Menz G, Tavernier J, Kay AB, Hamid Q, Membrane-bound and soluble alpha IL-5 receptor mRNA in the bronchial mucosa of atopic and nonatopic asthmatics. Am J Respir Crit Care Med 1997;155: 1413–18. [PubMed: 9105087]
5. Miyajima A, Mui AL, Ogorochi T, Sakamaki K, Receptors for granulocyte macrophage colony stimulating factor, interleukin-3, and interleukin-5. Blood 1993;82: 1960–74. [PubMed: 8400249]
6. Kampfer SS, Odermatt A, Dahinden CA, Fux M, Late IL-3-induced phenotypic and functional alterations in human basophils require continuous IL-3 receptor signaling. Journal of Leukocyte Biology 2017;101: 227–38. [PubMed: 27443880]
7. Hassani M, Koenderman L, Immunological and hematological effects of IL-5(Ralpha)-targeted therapy: An overview. Allergy 2018;73: 1979–88. [PubMed: 29611207]
8. Flood-Page PT, Menzies-Gow AN, Kay AB, Robinson DS, Eosinophil's role remains uncertain as anti-interleukin-5 only partially depletes numbers in asthmatic airway. Am J Respir Crit Care Med 2003;167: 199–204. [PubMed: 12406833]
9. Laviolette M, Gossage DL, Gauvreau G, Leigh R, Olivenstein R, Katial R, Busse WW, Wenzel S, Wu Y, Datta V, Kolbeck R, Molfino NA, Effects of benralizumab on airway eosinophils in asthmatic patients with sputum eosinophilia. J Allergy Clin Immunol 2013;132: 1086–96 e5. [PubMed: 23866823]
10. Kelly EA, Esnault S, Liu LY, Evans MD, Johansson MW, Mathur S, Mosher DF, Denlinger LC, Jarjour NN, Mepolizumab attenuates airway eosinophil numbers, but not their functional phenotype, in asthma. Am J Respir Crit Care Med 2017;196: 1385–95. [PubMed: 28862877]
11. Cheng JF, Ott NL, Peterson EA, George TJ, Hukee MJ, Gleich GJ, Leiferman KM, Dermal eosinophils in atopic dermatitis undergo cytolytic degeneration. J Allergy Clin Immunol 1997;99: 683–92. [PubMed: 9155836]
12. Erjefält JS, Andersson M, Greiff L, Korsgren M, Gizycki M, Jeffery PK, Persson GA, Cytolysis and piecemeal degranulation as distinct modes of activation of airway mucosal eosinophils. J Allergy Clin Immunol 1998;102: 286–94. [PubMed: 9723674]
13. Erjefält JS, Greiff L, Andersson M, Matsson E, Petersen H, Linden M, Ansari T, Jeffery PK, Persson CG, Allergen-induced eosinophil cytolysis is a primary mechanism for granule protein release in human upper airways. Am J Respir Crit Care Med 1999;160: 304–12. [PubMed: 10390416]
14. Erjefält JS, Korsgren M, Nilsson MC, Sundler F, Persson CG, Association between inflammation and epithelial damage-restitution processes in allergic airways in vivo. Clin Exp Allergy 1997;27: 1344–55. [PubMed: 9420140]
15. Uller L, Andersson M, Greiff L, Persson CG, Erjefalt JS, Occurrence of apoptosis, secondary necrosis, and cytolysis in eosinophilic nasal polyps. Am J Respir Crit Care Med 2004;170: 742–7. [PubMed: 15229095]
16. Neves JS, Perez SA, Spencer LA, Melo RC, Reynolds L, Ghiran I, Mahmudi-Azer S, Odemuyiwa SO, Dvorak AM, Moqbel R, Weller PF, Eosinophil granules function extracellularly as receptor-mediated secretory organelles. Proceedings of the National Academy of Sciences of the United States of America 2008;105: 18478–83. [PubMed: 19017810]
17. Yousefi S, Sharma SK, Stojkov D, Germic N, Aeschlimann S, Ge MQ, Flayer CH, Larson ED, Redai IG, Zhang S, Koziol-White CJ, Kariko K, Simon HU, Haczku A, Oxidative damage of SP-D

abolishes control of eosinophil extracellular DNA trap formation. Journal of Leukocyte Biology 2018;104: 205–14. [PubMed: 29733456]

18. Muniz VS, Silva JC, Braga YAV, Melo RCN, Ueki S, Takeda M, Hebisawa A, Asano K, Figueiredo RT, Neves JS, Eosinophils release extracellular DNA traps in response to Aspergillus fumigatus. J Allergy Clin Immunol 2018;141: 571–85 e7. [PubMed: 28943470]
19. Ueki S, Melo RC, Ghiran I, Spencer LA, Dvorak AM, Weller PF, Eosinophil extracellular DNA trap cell death mediates lytic release of free secretion-competent eosinophil granules in humans. Blood 2013;121: 2074–83. [PubMed: 23303825]
20. Yousefi S, Gold JA, Andina N, Lee JJ, Kelly AM, Kozlowski E, Schmid I, Straumann A, Reichenbach J, Gleich GJ, Simon HU, Catapult-like release of mitochondrial DNA by eosinophils contributes to antibacterial defense. Nat Med 2008;14: 949–53. [PubMed: 18690244]
21. Persson EK, Verstraete K, Heyndrickx I, Gevaert E, Aegerter H, Percier JM, Deswarte K, Verschueren KHG, Dansercoer A, Gras D, Chanez P, Bachert C, Goncalves A, Van Gorp H, De Haard H, Blanchetot C, Saunders M, Hammad H, Savvides SN, Lambrecht BN, Protein crystallization promotes type 2 immunity and is reversible by antibody treatment. Science 2019;364. [PubMed: 31624212]
22. Radonjic-Hoesli S, Wang X, de Graauw E, Stoeckle C, Styp-Rekowska B, Hlushchuk R, Simon D, Spaeth PJ, Yousefi S, Simon HU, Adhesion-induced eosinophil cytolysis requires the receptor-interacting protein kinase 3 (RIPK3)-mixed lineage kinase-like (MLKL) signaling pathway, which is counterregulated by autophagy. J Allergy Clin Immunol 2017;140: 1632–42. [PubMed: 28412393]
23. Esnault S, Johansson MW, Kelly EA, Koenderman L, Mosher DF, Jarjour NN, IL-3 up-regulates and activates human eosinophil CD32 and alphaMbeta2 integrin causing degranulation. Clin Exp Allergy 2017;47: 488–98. [PubMed: 28000949]
24. Esnault S, Kelly EA, Shen ZJ, Johansson MW, Malter JS, Jarjour NN, IL-3 maintains activation of the p90S6K/RPS6 pathway and increases translation in human eosinophils. J Immunol 2015;195: 2529–39. [PubMed: 26276876]
25. Liu LY, Sedgwick JB, Bates ME, Vrtis RF, Gern JE, Kita H, Jarjour NN, Busse WW, Kelly EAB, Decreased expression of membrane IL-5R alpha on human eosinophils: I. Loss of membrane IL-5 alpha on eosinophils and increased soluble IL-5R alpha in the airway after antigen challenge. J Immunol 2002;169: 6452–58. [PubMed: 12444154]
26. Liu LY, Sedgwick JB, Bates ME, Vrtis RF, Gern JE, Kita H, Jarjour NN, Busse WW, Kelly EAB, Decreased expression of membrane IL-5R alpha on human eosinophils: II. IL-5 down-modulates its receptor via a proteinase-mediated process. J Immunol 2002;169: 6459–66. [PubMed: 12444155]
27. Esnault S, Bernau K, Torr EE, Bochkov YA, Jarjour NN, Sandbo N, RNA-sequencing analysis of lung primary fibroblast response to eosinophil-degranulation products predicts downstream effects on inflammation, tissue remodeling and lipid metabolism. Respir Res 2017;18: 188. [PubMed: 29126429]
28. Kaneko M, Horie S, Kato M, Gleich GJ, Kita H, A crucial role for beta 2 integrin in the activation of eosinophils stimulated by IgG. J Immunol 1995;155: 2631–41. [PubMed: 7544379]
29. Kaneko M, Swanson MC, Gleich GJ, Kita H, Allergen-specific IgG1 and IgG3 through Fc gamma RII induce eosinophil degranulation. J Clin Invest 1995;95: 2813–21. [PubMed: 7769121]
30. Peebles RS Jr., Liu MC, Lichtenstein LM, Hamilton RG, IgA, IgG and IgM quantification in bronchoalveolar lavage fluids from allergic rhinitics, allergic asthmatics, and normal subjects by monoclonal antibody-based immunoenzymetric assays. J Immunol Methods 1995;179: 77–86. [PubMed: 7868927]
31. Nahm DH, Kim HY, Park HS, Elevation of specific immunoglobulin A antibodies to both allergen and bacterial antigen in induced sputum from asthmatics. Eur Respir J 1998;12: 540–5. [PubMed: 9762776]
32. Mukherjee M, Bulir DC, Radford K, Kjarsgaard M, Huang CM, Jacobsen EA, Ochkur SI, Catuneanu A, Lamothe-Kipnes H, Mahony J, Lee JJ, Lacy P, Nair PK, Sputum autoantibodies in patients with severe eosinophilic asthma. J Allergy Clin Immunol 2017.

33. Uy B, McGlashan SR, Shaikh SB, Measurement of reactive oxygen species in the culture media using Acridan Lumigen PS-3 assay. Journal of biomolecular techniques : JBT 2011;22: 95–107. [PubMed: 21966257]
34. Bernau K, Torr EE, Evans MD, Aoki JK, Ngam CR, Sandbo N, Tensin 1 is essential for myofibroblast differentiation and extracellular matrix formation. Am J Respir Cell Mol Biol 2017;56: 465–76. [PubMed: 28005397]
35. Johansson MW, Annis DS, Mosher DF, alpha(M)beta(2) integrin-mediated adhesion and motility of IL-5-stimulated eosinophils on periostin. Am J Respir Cell Mol Biol 2013;48: 503–10. [PubMed: 23306834]
36. Barretto KT, Swanson CM, Nguyen CL, Annis DS, Esnault SJ, Mosher DF, Johansson MW, Control of cytokine-driven eosinophil migratory behavior by TGF-beta-induced protein (TGFBI) and periostin. PloS one 2018;13: e0201320. [PubMed: 30048528]
37. Johansson MW, Khanna M, Bortnov V, Annis DS, Nguyen CL, Mosher DF, IL-5-stimulated eosinophils adherent to periostin undergo stereotypic morphological changes and ADAM8-dependent migration. Clin Exp Allergy 2017;47: 1263–74. [PubMed: 28378503]
38. Melo RCN, Weller PF, Contemporary understanding of the secretory granules in human eosinophils. Journal of Leukocyte Biology 2018;104: 85–93. [PubMed: 29749658]
39. Spencer LA, Bonjour K, Melo RC, Weller PF, Eosinophil secretion of granule-derived cytokines. Front Immunol 2014;5: 496. [PubMed: 25386174]
40. Nagata M, Sedgwick JB, Kita H, Busse WW, Granulocyte-macrophage colony-stimulating factor augments ICAM-1 and VCAM-1 activation of eosinophil function. Am J Resp Cell Mol Biol 1998;19: 158–66.
41. Andersen SS, Spindle assembly and the art of regulating microtubule dynamics by MAPs and Stathmin/Op18. Trends in cell biology 2000;10: 261–7. [PubMed: 10856928]
42. Uchida S, Shumyatsky GP, Deceivingly dynamic: Learning-dependent changes in stathmin and microtubules. Neurobiology of learning and memory 2015;124: 52–61. [PubMed: 26211874]
43. Filbert EL, Le Borgne M, Lin J, Heuser JE, Shaw AS, Stathmin regulates microtubule dynamics and microtubule organizing center polarization in activated T cells. J Immunol 2012;188: 5421–7. [PubMed: 22529300]
44. Esnault S, Hebert AS, Jarjour NN, Coon JJ, Mosher DF, Proteomic and Phosphoproteomic Changes Induced by Prolonged Activation of Human Eosinophils with IL-3. Journal of proteome research 2018;17: 2102–11. [PubMed: 29706072]
45. Wilkerson EM, Johansson MW, Hebert AS, Westphall MS, Mathur SK, Jarjour NN, Schwantes EA, Mosher DF, Coon JJ, The peripheral blood eosinophil proteome. Journal of proteome research 2016;15: 1524–33. [PubMed: 27005946]
46. Amano M, Nakayama M, Kaibuchi K, Rho-kinase/ROCK: A key regulator of the cytoskeleton and cell polarity. Cytoskeleton 2010;67: 545–54. [PubMed: 20803696]
47. Alblas J, Ulfman L, Hordijk P, Koenderman L, Activation of Rhoa and ROCK are essential for detachment of migrating leukocytes. Mol Biol Cell 2001;12: 2137–45. [PubMed: 11452009]
48. Goedert M, Cuenda A, Craxton M, Jakes R, Cohen P, Activation of the novel stress-activated protein kinase SAPK4 by cytokines and cellular stresses is mediated by SKK3 (MKK6); comparison of its substrate specificity with that of other SAP kinases. EMBO J 1997;16: 3563–71. [PubMed: 9218798]
49. Eyers PA, Craxton M, Morrice N, Cohen P, Goedert M, Conversion of SB 203580-insensitive MAP kinase family members to drug-sensitive forms by a single amino-acid substitution. Chemistry & biology 1998;5: 321–8. [PubMed: 9653550]
50. Koenderman L, van der Bruggen T, Schweizer RC, Warringa RA, Coffer P, Caldenhoven E, Lammers JWJ, Raaijmakers JA, Eosinophil priming by cytokines: from cellular signal to in vivo modulation. European Respiratory Journal 1996;9: 119s–25s.
51. Luijk B, Lindemans CA, Kanters D, van der Heijde R, Bertics P, Lammers JW, Bates ME, Koenderman L, Gradual increase in priming of human eosinophils during extravasation from peripheral blood to the airways in response to allergen challenge. J Allergy Clin Immunol 2005;115: 997–1003. [PubMed: 15867857]

52. Bates ME, Sedgwick JB, Zhu Y, Liu LY, Heuser RG, Jarjour NN, Kita H, Bertics PJ, Human airway eosinophils respond to chemoattractants with greater eosinophil-derived neurotoxin release, adherence to fibronectin, and activation of the Ras-ERK pathway when compared with blood eosinophils. J Immunol 2010;184: 7125–33. [PubMed: 20495064]
53. Johansson MW, Mosher DF, Integrin activation states and eosinophil recruitment in asthma. Frontiers in Pharmacology 2013;4: 33. [PubMed: 23554594]
54. Sano M, Leff AR, Myou S, Boetticher E, Meliton AY, Learoyd J, Lambertino AT, Munoz NM, Zhu X, Regulation of interleukin-5-induced beta2-integrin adhesion of human eosinophils by phosphoinositide 3-kinase. Am J Respir Cell Mol Biol 2005;33: 65–70. [PubMed: 15802551]
55. Barthel SR, Annis DS, Mosher DF, Johansson MW, Differential engagement of modules 1 and 4 of vascular cell adhesion molecule-1 (CD106) by integrins alpha4beta1 (CD49d/29) and alphaMbeta2 (CD11b/18) of eosinophils. J Biol Chem 2006;281: 32175–87. [PubMed: 16943205]
56. Omoi NO, Arai M, Saito M, Takatsu H, Shibata A, Fukuzawa K, Sato K, Abe K, Fukui K, Urano S, Influence of oxidative stress on fusion of pre-synaptic plasma membranes of the rat brain with phosphatidyl choline liposomes, and protective effect of vitamin E. Journal of nutritional science and vitaminology 2006;52: 248–55. [PubMed: 17087050]
57. Lin WJ, Kuang HY, Oxidative stress induces autophagy in response to multiple noxious stimuli in retinal ganglion cells. Autophagy 2014;10: 1692–701. [PubMed: 25207555]
58. Fukui K, Reactive oxygen species induce neurite degeneration before induction of cell death. Journal of clinical biochemistry and nutrition 2016;59: 155–59. [PubMed: 27895381]
59. Han ST, Mosher DF, IL-5 induces suspended eosinophils to undergo unique global reorganization associated with priming. Am J Respir Cell Mol Biol 2014;50: 654–64. [PubMed: 24156300]
60. Mosher DF, Wilkerson EM, Turton KB, Hebert AS, Coon JJ, Proteomics of eosinophil activation. Frontiers in medicine 2017;4: 159. [PubMed: 29034237]
61. Bustos-Moran E, Blas-Rus N, Martin-Cofreces NB, Sanchez-Madrid F, Microtubule-associated protein-4 controls nanovesicle dynamics and T cell activation. J Cell Sci 2017;130: 1217–23. [PubMed: 28209780]
62. Li L, Hu J, He T, Zhang Q, Yang X, Lan X, Zhang D, Mei H, Chen B, Huang Y, P38/MAPK contributes to endothelial barrier dysfunction via MAP4 phosphorylation-dependent microtubule disassembly in inflammation-induced acute lung injury. Scientific reports 2015;5: 8895. [PubMed: 25746230]
63. Ramkumar A, Jong BY, Ori-McKenney KM, ReMAPping the microtubule landscape: How phosphorylation dictates the activities of microtubule-associated proteins. Dev Dyn 2018;247: 138–55. [PubMed: 28980356]
64. Livanos P, Galatis B, Apostolakos P, The interplay between ROS and tubulin cytoskeleton in plants. Plant signaling & behavior 2014;9: e28069. [PubMed: 24521945]
65. Shamri R, Young KM, Weller PF, Rho and Rac, but not ROCK, are required for secretion of human and mouse eosinophil-associated RNases. Clin Exp Allergy 2019;49: 190–98. [PubMed: 30295352]
66. Weiler CR, Kita H, Hukee M, Gleich GJ, Eosinophil viability during immunoglobulin-induced degranulation. J Leukocyte Biol 1996;60: 493–501. [PubMed: 8864134]
67. Moss DK, Betin VM, Malesinski SD, Lane JD, A novel role for microtubules in apoptotic chromatin dynamics and cellular fragmentation. J Cell Sci 2006;119: 2362–74. [PubMed: 16723742]
68. Allen WE, Zicha D, Ridley AJ, Jones GE, A role for Cdc42 in macrophage chemotaxis. J Cell Biol 1998;141: 1147–57. [PubMed: 9606207]

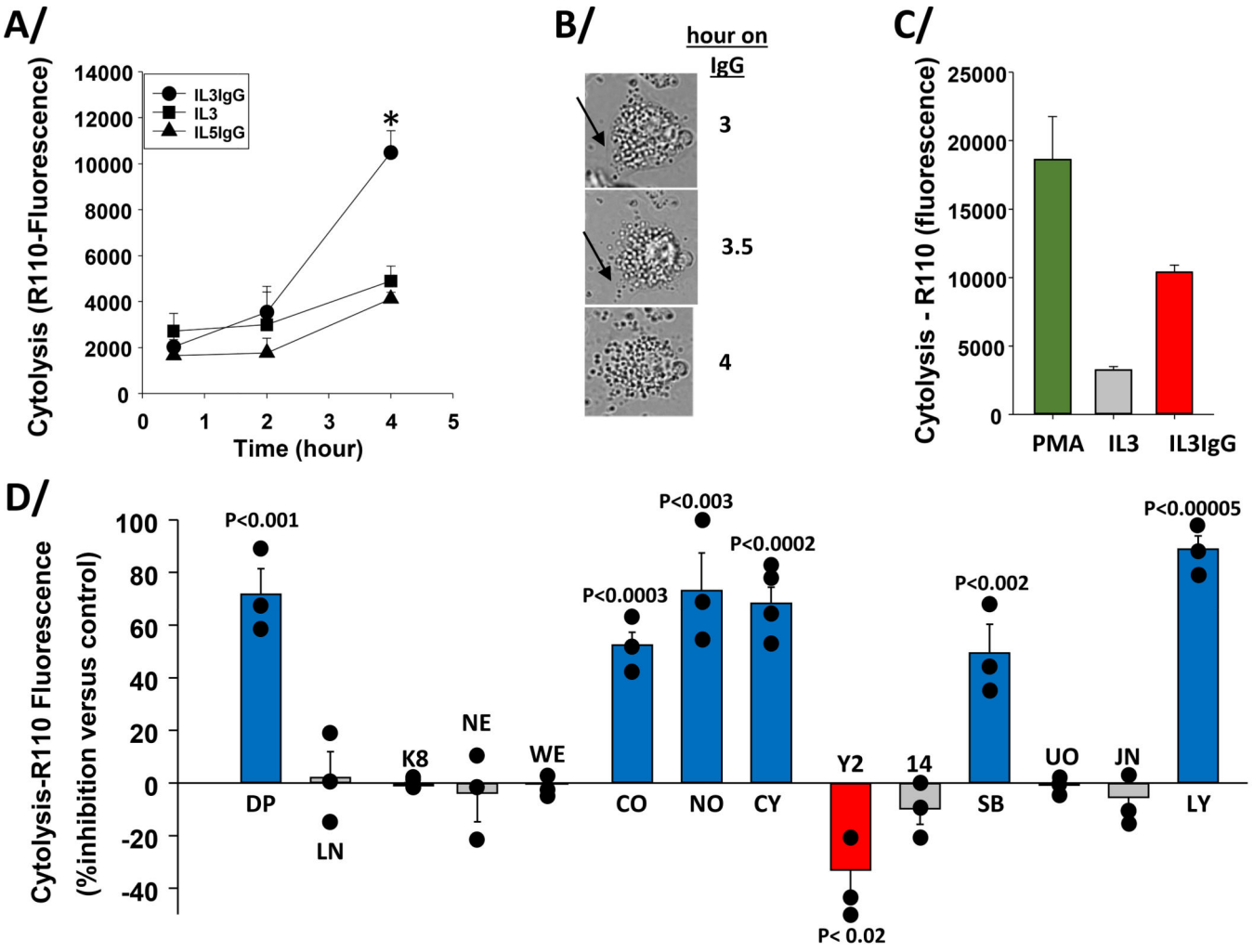

Inhibitor (conc.)	Target
DP: Diphenyleneiodonium (DPI; 5μM)	Nicotinamide adenine dinucleotide phosphate (NADPH)-oxidase (ROS production)
LN: L-NMMA (10μM)	Nitric oxide synthase
K8: GSK843 (10μM)	Receptor-interacting serine/threonine-protein kinase 3 (RIPK3) (Necroptosis)
NE: Necrosulfonamide (10μM)	Mixed lineage kinase domain-like (MLKL) (Necroptosis)
WE: Z-WEHD-FMK (5μM)	Caspase-1
CO: Colchicine (1μM)	Microtubule polymerization

Inhibitor (conc.)	Target
NO: Nocodazole (1μM)	Microtubule polymerization
CY: Cytochalasin-D (1μM)	Actin polymerization formation
Y2: Y27632 (10μM)	Rho-associated, coiled-coil containing protein kinase (ROCK)
14: 14-22-amide (4μM)	Protein Kinase A (PKA)
SB: SB203580 (0.5μM)	P38 mitogen-activated protein kinase (p-38)
U0: U0126 (2μM)	Extracellular-signal-regulated kinase (ERK)
JN: JNK inhibitor II (5μM)	c-Jun N-terminal kinase (JNK)
LY: LY294002 (10μM)	Phosphatidylinositol 3-kinase (PI3K)

Figure 1. Inhibitor screens indicate that cytolysis of IL3-primed eosinophils on IgG requires ROS production, microtubule and actin polymerization, p38, and PI3K activity, and is favored by reduction of ROCK signaling.

Eosinophils were primed with IL3 and with IL5 (2 ng/ml) for 20 hours and seeded on heat-aggregated IgG (IL3IgG and IL5IgG) or without IgG (IL3) for the indicated times. **A/** Bis-AAF-R110 substrate was then added for 30 minutes and fluorescence was measured at $485nm_{Ex}/520nm_{Em}$. Cytolysis was significantly induced on IgG versus no IgG (IL3) at 4 hours (* *t*-test, p=0.003, n=4, IL3 versus IL3IgG). **B/** Images from time-lapse microscopy of IL3-primed eosinophils on IgG for the indicated times. Black arrow shows apparently intact cytoplasmic membrane at 3 hours and cytoplasmic membrane disruption starting at 3.5

hours. **C/** Eosinophil cytolysis at 4 hours under IL3IgG and IL3 conditions were compared to maximum cytolysis using PMA (100 ng/ml) for 4 hours. There was a statistically significant difference among the three conditions (ANOVA, $p<0.002$, $n=6$). **A/** and **C/** means ± standard error of the mean (SEM) are shown. **D/** Eosinophils were primed with IL3 (2 ng/ml) for 20 hours and were treated with the indicated inhibitors for 15 minutes before seeding on IgG for 5 h. Bis-AAF-R110 substrate was then added for 30 min and fluorescence was measured. Data are presented as percentage (%) inhibition of cytolysis versus each respective inhibitor vehicle or analog (mean ± SEM). Treatments with unadjusted statistically significant changes compared to their specific control are colored (blue and red) and *p* values are indicated on the graph (n=3 to 4 subjects per condition). Inhibitor names, final concentrations (conc.) and targets are shown in table below the graph.

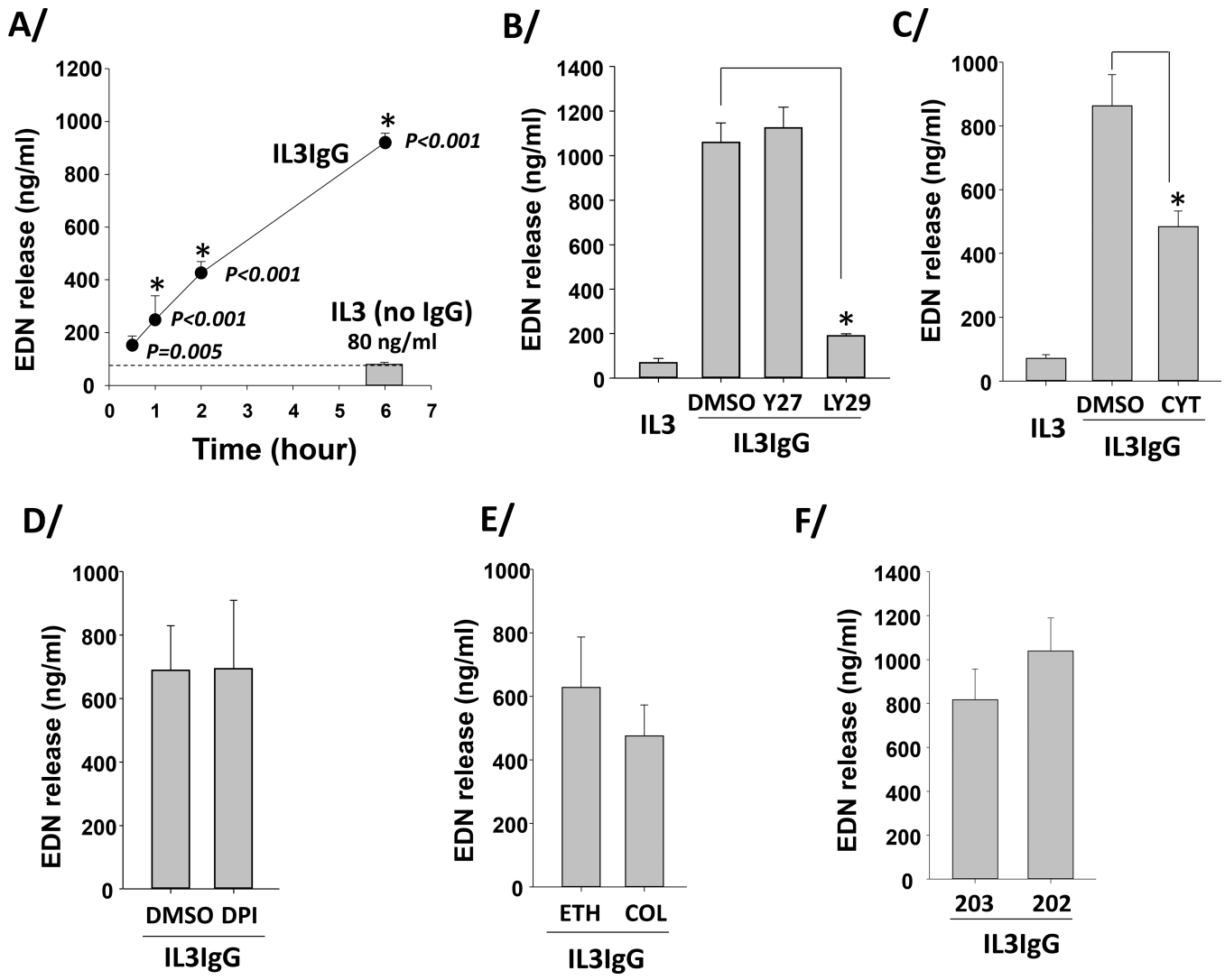

Figure 2. IL3-primed eosinophils degranulate early and continuously on IgG, independently of ROS production, microtubule polymerization, and ROCK and p38 signaling.

Eosinophils were primed with IL3 (2 ng/ml) for 20 hours and were seeded on IgG (IL3IgG) or without IgG (IL3). EDN released from eosinophils (degranulation) was measured by ELISA. **A/** EDN release at the different time-points on IgG (IL3IgG) were compared to EDN release when eosinophils were not on IgG for 6 hours (IL3, no IgG; mean=80 ng/ml, n=6). ANOVA was performed and *p* values are indicated on the graph for each time-point. *indicates that EDN release is statistically different from the release at 0.5 hour on IgG (n=6 for all time-points, ANOVA). Means ± SEM are shown. **B/C/D/E/F/** Eosinophils were primed with IL3 (2 ng/ml) for 20 hours and were treated with the indicated inhibitors, and vehicles or an analog control, (as used in Figure 1D) 15 min before seeded on IgG (IL3IgG). EDN released was measured after 4–5 h on IgG. Y27632 (Y27), LY294002 (LY29), cytochalasin-D (CYT) or diphenyleneiodonium (DPI) was compared to treatment with dimethyl sulfoxide (DMSO). Colchicine (COL) was compared to its vehicle, ethanol (ETH), and SB203850 (203) was compared to its analog control, SB202474 (202). *indicates that treatment is statistically significant from its vehicle (*t* test, $p<0.05$, n=3–4).

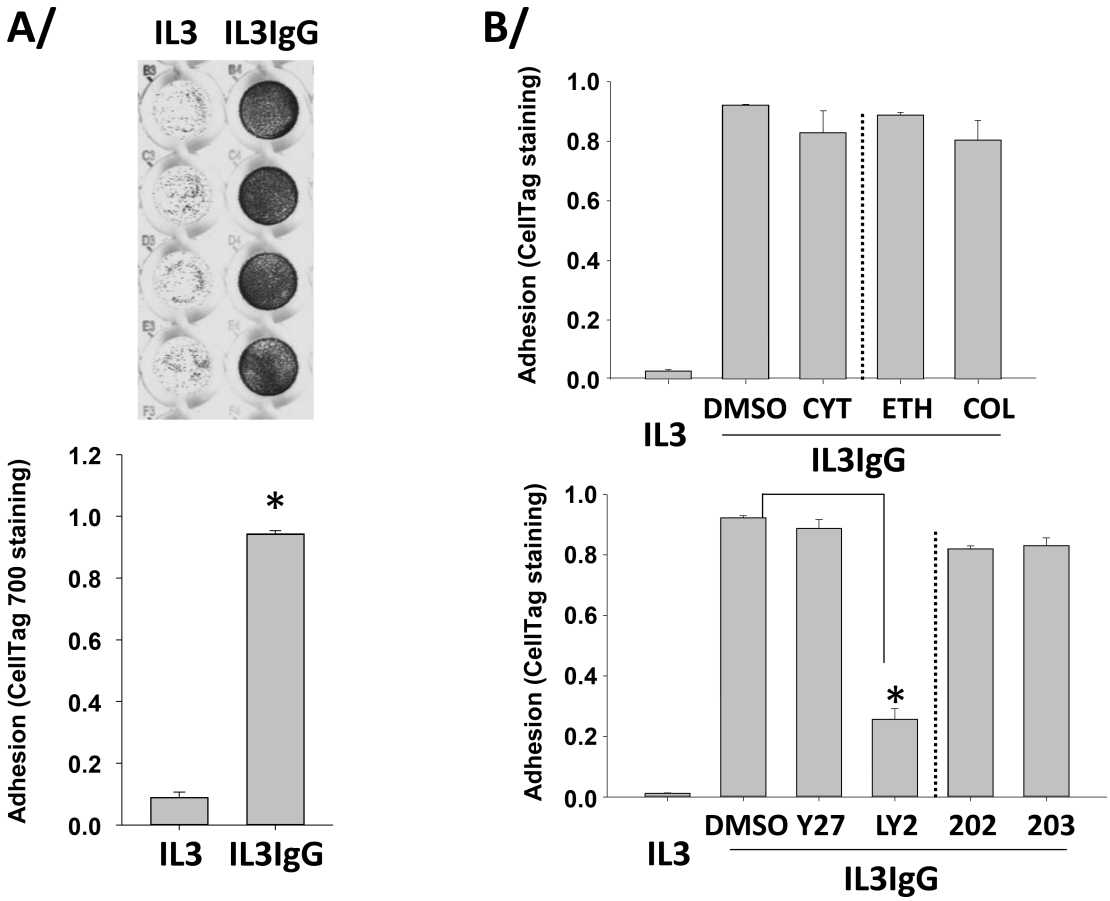

Figure 3. IL3-primed eosinophils adhere to IgG-coated surface in the presence of inhibitors of ROS production, microtubule formation, actin polymerization, or ROCK or p38 signaling.

Eosinophils were primed with IL3 (2 ng/ml) for 20 hours and were seeded on IgG (IL3IgG) or without IgG (IL3) for 2 hours. Then, eosinophils were stained using a non-specific cell stain, CellTag 700 Stain, to quantify the number of adherent cells. Non-adherent cells were washed away and fluorescence from the adherent cells was measured. **A/** On the top, representative wells in quadruplicate are shown for both IL3 and IL3IgG conditions. On the bottom, graph shows means ± SEM of quantified fluorescence from four experiments. Adhesion under IL3IgG and IL3 conditions was compared using paired *t* test ($p<0.001$, n=4). **B/** Eosinophils were primed with IL3 for 20 hours and treated with the indicated inhibitors for 15 minutes before seeding on IgG for 2 hours. Actin polymerization and ROCK inhibitors, **cytochalasin**-D (CYT) and Y27632 (Y27) did not affect adhesion compared to DMSO. The microtubule polymerization inhibitor, colchicine (COL) did not affect adhesion compared to its vehicle, ethanol (ETH). The p-38 inhibitor, SB203850 did not affect adhesion compared to its analog control, SB202474. Conversely, the PI3K inhibitor, LY294002 blocked adhesion. *indicates that adhesion is statistically different from DMSO ($p<0.001$, n=3; ANOVA).

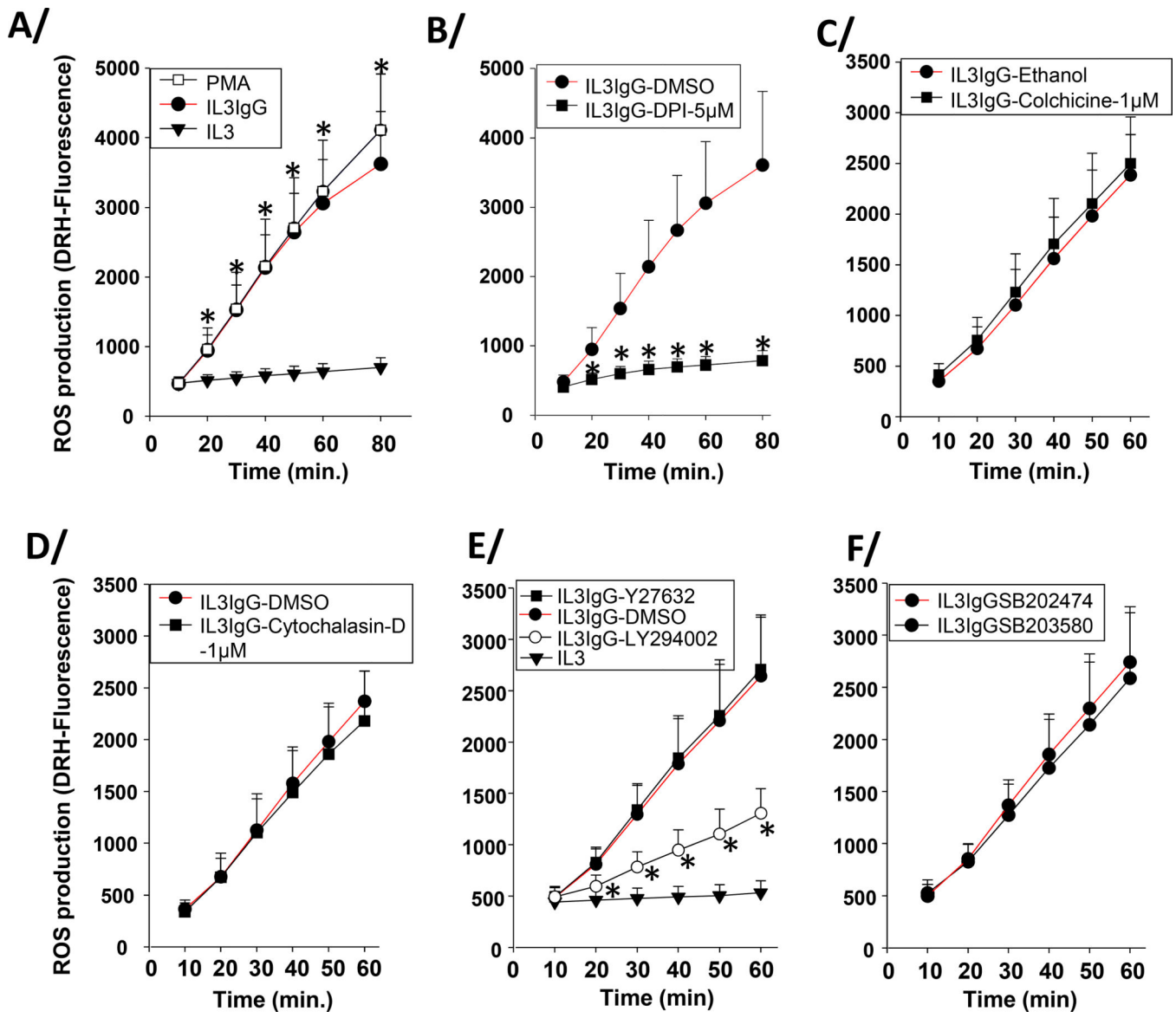

Figure 4. IL3-primed eosinophils produce ROS on IgG-coated surface in the presence of inhibitors of microtubule formation, actin polymerization, or ROCK or p38 signaling.

Eosinophils were primed with IL3 (2 ng/ml) for 20 hours. In the last hour of priming, eosinophils were incubated with dihydrorhodamine (DRH)-123 (5μM). Then, cells were seeded on IgG (IL3IgG) or without IgG (IL3). Intracellular ROS production was measured by fluorescence ($485nm_{Ex}/520nm_{Em}$) at the indicated time-points. **A/** ROS was measured under IL3 and IL3IgG conditions from 10 to 80 minutes. As a positive control for ROS production, IL3-primed eosinophils were treated with PMA (100 ng/ml) for the indicated times. *indicates statistically significant differences ($p<0.05$) between IL3IgG and IL3 at the indicated time points (paired *t* test, n=4). **B/C/D/E/F** Eosinophils were treated with inhibitors or vehicle only or analog control 15 minutes before seeding on IgG. **B/** * indicates that diphenyleneiodonium (DPI; 5μM) inhibits ROS production at each time-point compared to vehicle alone (IL3IgG-DMSO) (paired *t* test, $p<0.05$, n=3). ROS production was

independent of colchicine (**C**) and cytochalasin-D (**D**) treatments. **E**/ * indicates that LY294002 treatment inhibited ROS production at each time-point (paired *t* test, $p<0.05$, n=3). ROS production is independent of Y27632 (**E**) and SB203580 (**F**) treatments.

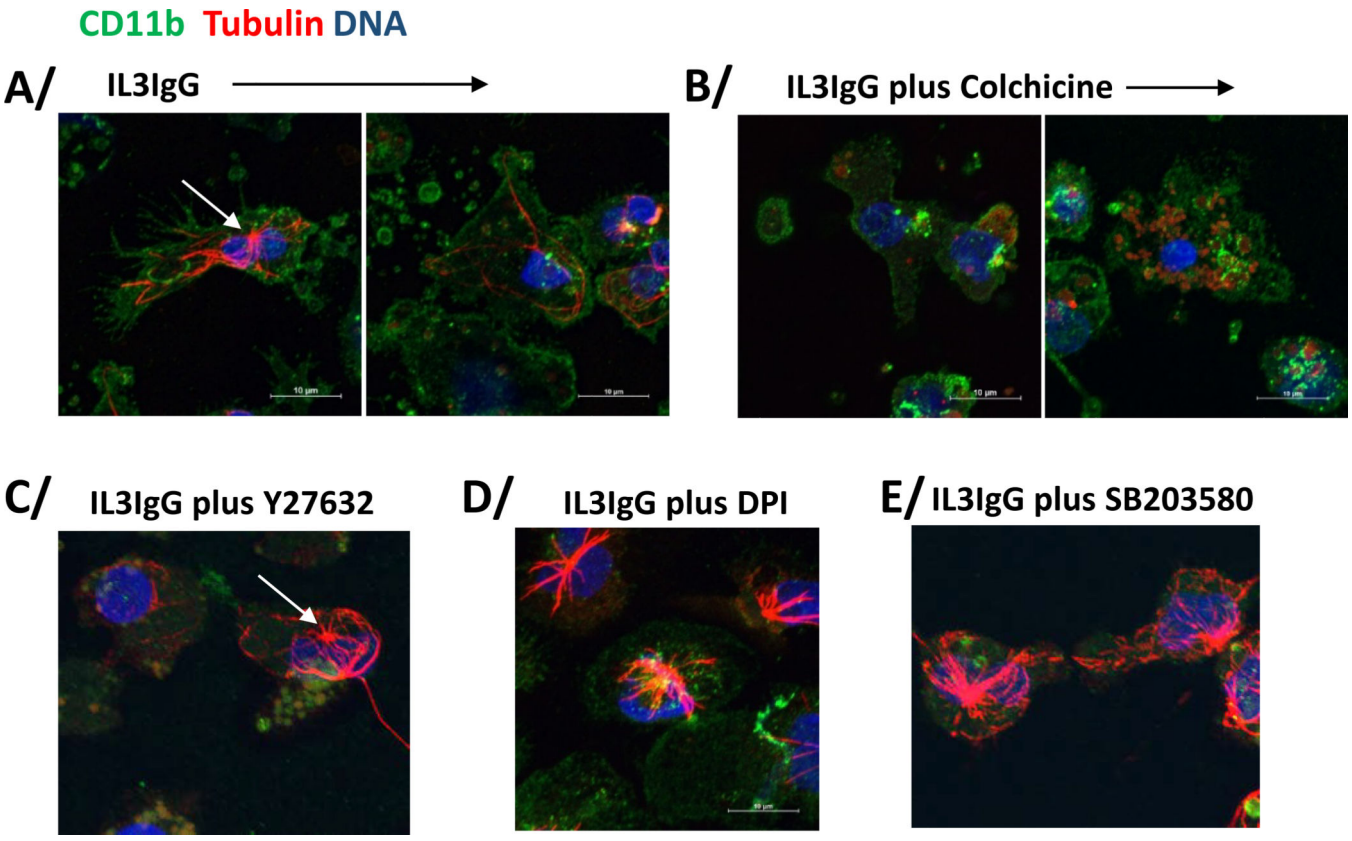

Figure 5. IL3-primed eosinophils display microtubule arrays on IgG-coated surface in the presence of inhibitors of ROCK, ROS production or p38 signaling.

Eosinophils were primed with IL3 (2 ng/ml) for 20 hours, treated with inhibitors or vehicle alone, and seeded on IgG for 4 hours. Eosinophils were stained for a membrane marker (CD11b; green), α-tubulin (red) and DNA (blue). **A/** Microtubule organization center (MTOC) is indicated by a white arrow. In the IL3IgG condition, two images are shown depicting two apparently different stages of eosinophil toward cytolysis. In the left image, the eosinophil appears spreading and still intact, and displays microtubule arrays. On the right, the eosinophil loses its microtubule arrays and its intact membrane. **B/** Colchicine treatment blocks microtubule array formation. **C/D/E/** Microtubule array formation was not inhibited by Y27632, DPI (ROS production) or SB203580 treatments.

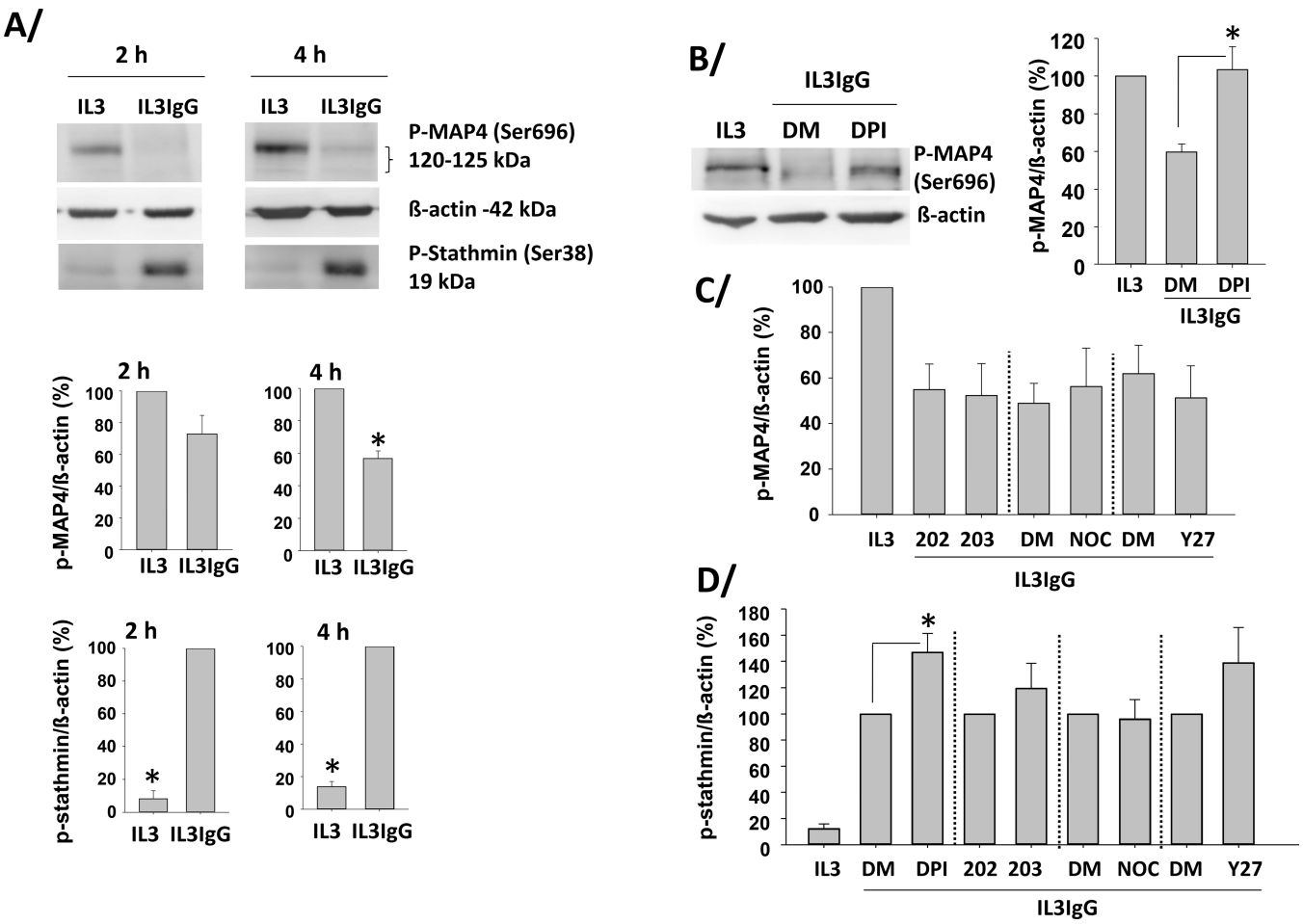

Figure 6. IL3-primed eosinophils display stathmin phosphorylation and MAP4 dephosphorylation on IgG.

Eosinophils were primed with IL3 (2 ng/ml) for 20 hours and were seeded on IgG (IL3IgG) or without IgG (IL3) for the indicated times. **A/** representative blots are shown and graphs represent the mean ± SEM of the indicated ratios after 2 and 4 hours on IgG, with IL3 for phospho-MAP4/ß-actin and IL3IgG for phospho-stathmin/ß-actin fixed at 100. *indicates statistical differences $p<0.002$ to $p<0.00003$ between IL3 and IL3IgG for n=3 to 4 different eosinophil donors (paired *t* test). **B/C/D** after IL3 priming, eosinophils were treated with the indicated inhibitors (DPI, SB203580 (203), nocodazole (NOC), and Y27632 (Y27)) or their respective vehicle (DMSO; DM) or analog control (SB202474; 202) for 10 minutes before seeding on IgG for 3.75 hours. **B/** a representative blot is shown for inhibition of ROS production (DPI) and graph represents the mean ± SEM using eosinophils from 3 different subjects with IL3 fixed at 100. *indicates that DPI treatment increases MAP4 phosphorylation compared to DMSO ($p<0.03$, paired *t* test). **C/** No other inhibitor changed MAP4 phosphorylation status (n=3). **D/** *DPI increased stathmin phosphorylation compared to DMSO ($p<0.05$, paired *t* test, n=3).

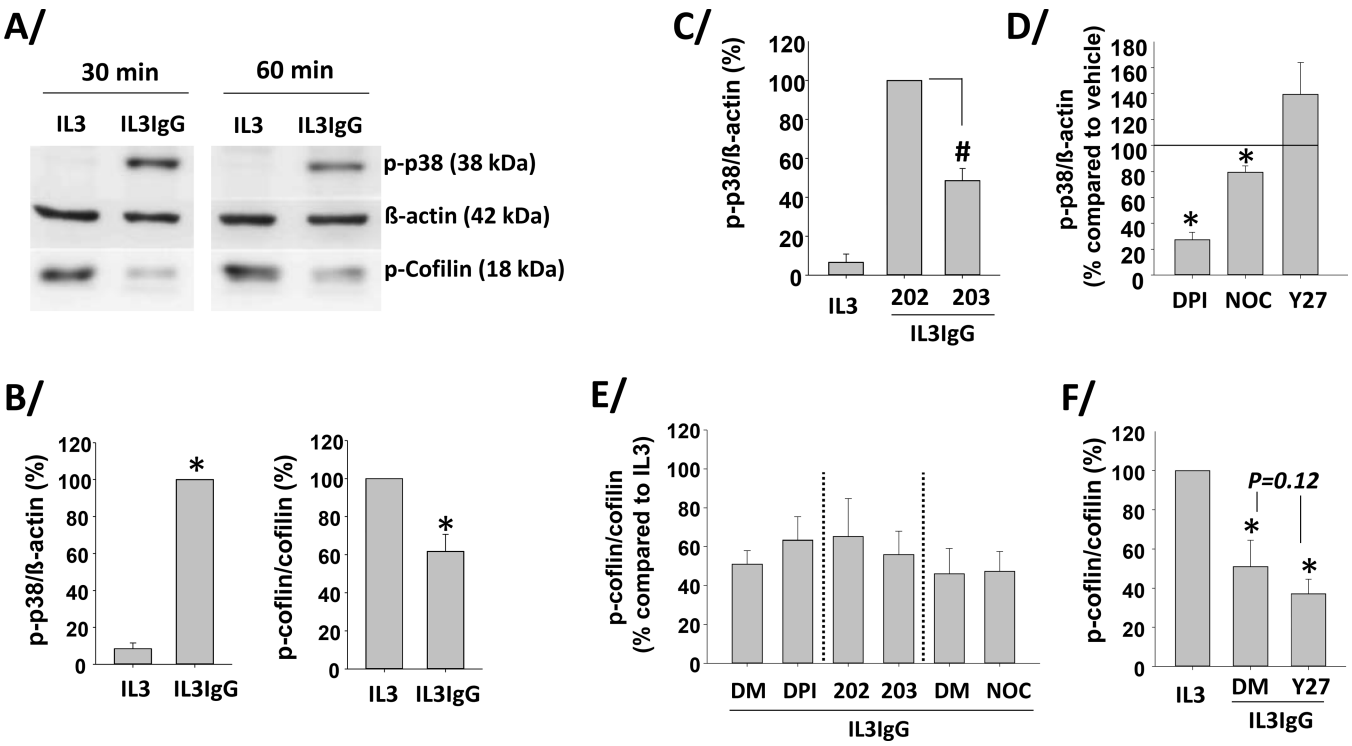

Figure 7. IL3-primed eosinophils display ROS-dependent increased p-38 phosphorylation, and dephosphorylation of cofilin on IgG.

Eosinophils were primed with IL3 (2 ng/ml) for 20 hours and were seeded (IL3IgG) or not (IL3) on IgG for the indicated times. Phosphorylation of p-38 (p-p38) and cofilin (p-cofilin) were analyzed by western-blot. **A/** representative blots. **B/** graphs represent the mean ± SEM of the indicated ratios after 60 minutes on IgG, with IL3IgG for p-p38/ß-actin and IL3 for p-cofilin/cofilin fixed at 100. *indicates statistical differences between IL3 and IL3IgG (p-p38/ß-actin, $p<0.00005$, n=4; and p-cofilin/cofilin, $p<0.007$, n=5, paired *t* test). **C/D/E/F/** the indicated inhibitors or their specific vehicle only or analog control was added after IL3 priming and 10 minutes before cells were seeded on IgG for 60 minutes. **C/** #SB203580 (203) inhibited IgG-induced p-p38 compared to its analog control, SB202474 fixed at 100 (ANOVA, $p<0.001$, n=3). **D/** DPI, nocodazole (NOC), and Y27632 effects on p-p38 were compared to their respective vehicles used as control and fixed at 100. *indicates statistical significant change compared to control (paired *t* test, $p<0.05$, n=3). **E/** DPI, SB203580 (203) and nocodazole (NOC) did not affect cofilin phosphorylation compare to DMSO (DM) or the analog, SB202474 (202) fixed at 100 (paired *t* test, n=3). **F/** *indicates cofilin dephosphorylation compared to IL3, which is fixed at 100 (no IgG) (ANOVA, $p<0.02$ for DMSO only (DM) and $p<0.007$ for Y27632 (Y27), n=3).